ARTICLE
Journal of Cellular Biochemistry 112:2307–2316 (2011)

Journal of Cellular Biochemistry

Cigarette Smoke-Induced Skeletal Muscle Atrophy is Associated with Up-Regulation of USP-19 via p38 and ERK MAPKs

Qian Liu,[1] Wei-Guo Xu,[1] Yong Luo,[1] Feng-Feng Han,[1] Xiao-Hong Yao,[2] Tian-Yun Yang,[1] Yue Zhang,[1] Wei-Feng Pi,[1] and Xue-Jun Guo[1*]

[1]*Department of Respirology, College of Medicine, Xinhua Hospital, Shanghai Jiao Tong University, Shanghai, China*
[2]*Department of Pathology, College of Medicine, Xinhua Hospital, Shanghai Jiao Tong University, Shanghai, China*

ABSTRACT

Ubiquitin-specific proteases (USPs) deubiquitinate ubiquitin–protein conjugates in the ubiquitin–proteasome system. Previous research shows that ubiquitin-specific protease-19 (USP-19) is up-regulated in mammalian skeletal muscle in some degradative conditions, such as including fasting, diabetes, dexamethasone treatment, and cancer, and its function is associated with muscle atrophy. However, it is still unclear whether USP-19 is involved in muscle atrophy induced by chronic obstructive pulmonary disease. Rats exposed to chronic cigarette smoke and L6 myotubes incubated with cigarette smoke extract (CSE) were studied here. Using western blot analysis and quantitative real-time polymerase chain reaction (qPCR), we observed over-expression of USP-19 and down-regulation of myosin heavy chain (MHC) in both models. Moreover, CSE exposure inhibited myogenic differentiation and myotube formation in L6 myotubes. To explore the mechanism underlying these effects, we investigated the levels of phosphorylated mitogen-activated protein kinases (MAPKs) and total MAPKs. Exposing myotubes to CSE resulted in the general activation of MAPKs such as p38, JNK, and ERK1/2. The ERK inhibitor PD98059 and the p38 inhibitor SB203580 significantly blocked the increase in USP-19 gene expression induced by CSE. Our findings suggest that USP-19 is associated with muscle atrophy in response to cigarette smoke and is a potential therapeutic target. CSE promotes myotube wasting in culture partly by inhibiting myogenic differentiation and acts via p38 and ERK MAPK to stimulate expression of USP-19 in vitro. J. Cell. Biochem. 112: 2307–2316, 2011.

KEY WORDS: UBIQUITIN-SPECIFIC PROTEASE-19; MUSCLE WASTING; L6 MYOTUBES; CIGARETTE SMOKE EXTRACT; MAPK PATHWAY

Chronic obstructive pulmonary disease (COPD) has been predicted to become the third leading cause of death and the fifth leading cause of disability in the world by 2020 [Coen et al., 1998]. Cigarette smoking is its primary risk factor [Churg et al., 2008]. Skeletal muscle weakness is of great clinical importance in COPD, as it is recognized to contribute independently to poor health status, increased healthcare utilization, and even mortality [Decramer et al., 1997]. Rapid loss of muscle protein, especially the contractile components, is believed to result from the activation of the ubiquitin–proteasome proteolytic pathway. Many studies have demonstrated the importance of enzymes that mediate ubiquitin conjugation in muscular atrophy. However, little is known about the role of deubiquitinating enzymes in this process.

In recent years, extensive research has shown that the loss of skeletal muscle proteins results from a negative balance between the rates of protein synthesis and protein breakdown. Several animal models of atrophy have established the involvement of the ubiquitin–proteasome pathway in muscular atrophy [Jagoe et al., 2002; Sacheck et al., 2007]. Components of the ubiquitin-conjugating apparatus are active in atrophying muscles, as indicated by elevated mRNA levels of E3 ubiquitin ligases such as muscle atrophy F-box (MAFbx, also known as Atrogin-1) and muscle ring finger 1 (MuRF1) [Bodine et al., 2001; Doucet et al., 2007] and elevated levels of ubiquitin-conjugated proteins. However, the role of deubiquitinating enzymes in muscle atrophy is not well understood. The ubiquitin-specific protease-19 (USP-19) gene is comprised of a total open reading frame of 4071 bp, encoding a 150-kDa protein with deconjugase activity. High level of USP-19 mRNA and protein expression are detected in the glycolytic extensor digitorum longus muscle of rats in some degradative conditions,

Qian Liu and Wei-Guo Xu contributed equally to this work.

Grant sponsor: Shanghai Natural Science Foundation Project; Grant number: 05ZR14063.

*Correspondence to: Xue-Jun Guo, PhD, Department of Respirology, College of Medicine, Xinhua Hospital, Shanghai Jiao Tong University, 1665 KongJiang Road, Shanghai 200092, China. E-mail: liuqian_1980@hotmail.com

Received 25 September 2010; Accepted 8 April 2011 • DOI 10.1002/jcb.23151 • © 2011 Wiley-Liss, Inc.
Published online 18 April 2011 in Wiley Online Library (wileyonlinelibrary.com).

including fasting, diabetes, dexamethasone treatment, and cancer [Combaret et al., 2005]. Sundaram et al. [2009] used small interfering RNA in L6 muscle cells to study the relationship between the expression of USP-19 and the major myofibrillar proteins. Depletion of USP-19 increases the expression of myosin heavy chain (MHC), myogenin (MyoG), troponin, and tropomyosin. These studies demonstrate that USP-19 modulates the transcription of major myofibrillar proteins and indicate that inhibition of USP-19 could be a novel therapeutic mechanism for the prevention and treatment of muscle protein catabolism. However, USP-19 gene expression and its role in muscle wasting in response to COPD have not been evaluated. Because of the overwhelming role of cigarette smoke (CS) as a causative agent and a lack of skeletal muscle cells in culture models based on cigarette smoke extract (CSE), which has been used to understand the precise molecular mechanisms of the disorders triggered and regulated by CS at the cellular level, rats exposed to chronic CS and L6 myotubes treated with various concentrations of CSE were chosen for our study. Comprehensive and complex effects of CSE on cell growth and biological function occur, and many signaling pathways are involved, including p38 [Pera et al., 2010], ERK1/2 [Pera et al., 2010; Shih et al., 2010], and JNK [Pera et al., 2010]. Moreover, MAPKs are important in the cellular mechanisms of the atrophic process induced by COPD, and p38 MAPK has been identified as a potential regulator of muscle catabolism [Tracey, 2002; Coulthard et al., 2009]. Therefore, we hypothesized that CS induces over-expression of USP-19 in skeletal muscle and that the MAPK pathways connect USP-19 to muscle atrophy.

Our results show that in vivo chronic CS and in vitro CSE incubation induced muscle atrophy, which were associated with the over-expression of USP-19, a factor believed to be crucial in the regulation of muscle protein metabolism. USP-19 up-regulation in response to CSE was associated with activation of all three major MAPKs; p38 and ERK1/2 appeared to be essential for USP-19 up-regulation, as specific inhibitors blocked increases in USP-19 protein expression.

MATERIALS AND METHODS

ANIMAL CIGARETTE SMOKE EXPOSURE

Adult male Sprague-Dawley (S-D) rats weighing 350 ± 10 g were purchased from the Chinese Academy of Sciences and housed under controlled environmental conditions (25°C, 12 h lighting per day). They were fed a commercial laboratory chow and water ad libitum before the experiments were performed. The local institutional animal care committees approved the animal facilities and protocols. All rats were divided into four exposure groups: (a) Sham-exposed (CTRL group) ($n = 6$), (b) 4 weeks CS ($n = 6$), (c) 8 weeks CS ($n = 6$), and (d) 12 weeks CS ($n = 6$). Rats were placed in 6-L perspex chambers (three rats/chamber) and exposed to 50 ml of smoke every 30 s with fresh air being pumped in for the remaining time. Each rat's whole body was exposed to CS generated from 20 DaQianMen cigarettes per day (ShangHai, China, 1.25 mg nicotine per cigarette) in 6-L smoking chambers (~90 min per exposure period). Sham-exposed animals were exposed to normal air under the same conditions. Rats were sacrificed by intra-peritoneal injection of 2.5% sodium pentobarbital [Stevenson et al., 2005].

HISTOLOGICAL ANALYSIS

For histological examination, the lungs and quadriceps femoris muscle (QFM) were immersed in 4% paraformaldehyde for 24 h, imbedded in paraffin, and stained with hematoxylin and eosin (H&E).

CELL CULTURE

L6 myoblasts (Chinese Academy of Sciences Cellbank) were grown in Dulbecco's modified Eagle's medium (DMEM) containing 10% FBS at 37°C in a humidified 5% CO_2, 95% air atmosphere in 96-well, 6-well, or 100-mm plates. Cells were grown to 80% confluence and induced to differentiate into multinucleated myotubes by reducing the FBS concentration to 2% for 4 days prior to experimentations (changing to fresh medium at 48 h) [Sultan et al., 2006]. CSE was added to differentiation media for incubation with myotubes. The cells were examined for evidence of myotube formation and growth with an inverted Olympus CK40-F200 microscope. To preserve the characteristics of the L6 cell line, cells were split a maximum of seven times.

CSE PREPARATION

CSE was prepared using a modified version of the method of Carp and Janoff [1978]. Briefly, a full-strength DaQianMen cigarette (filters removed) was combusted through a modified 50-ml syringe apparatus. The smoke was bubbled through 10 ml DMEM until the unburned butt was less than 1 cm long. Each cigarette yielded five draws of the syringe (to the 50 ml mark), with each individual draw taking approximately 10 s to complete. This solution represented "100%" strength. Smoked medium was then passed through a 0.25-μm filter to sterilize the solution. Smoked medium was diluted in DMEM to the required strength and used for the experiment within 30 min.

REVERSE TRANSCRIPTION AND COMPARATIVE ANALYSIS OF QUANTITATIVE REAL-TIME PCR (qPCR)

Total RNA was extracted from the QFM tissues and L6 cells using TRIzol reagent (Invitrogen) as described by the manufacturer. RNA (2 μg) was reverse-transcribed into cDNA using the PrimeScript RT reagent kit (Takara) with oligo(dT) and random hexamers as primers in a 20-μl final volume. Quantitative real-time polymerase chain reaction (qPCR) was then performed using an ABI Prism 7500 Sequence Detection System (Applied Biosystems) and SYBR Premix Ex Taq (Takara). Before qPCR, the efficiency of amplification was determined for each primer set. All primer sets exhibited an efficiency >90% as required for the ΔΔCt relative quantification algorithm. cDNA (30 ng/reaction) was used as a template. Cycling conditions were as follows: Step 1, 30 s at 95°C; step 2, 5 s at 95°C; and step 3, 34 s at 60°C, with 40 repeats of step 2 to step 3. For each sample, a value of the threshold cycle (Ct) was calculated based on the time changes in the mRNA expression level calculated subsequent to normalization with glyceraldehyde-3-phosphatede-

hydrogenase (GAPDH). The program calculates the ΔCt and the ΔΔCt using the formulas that are listed below: ΔCt = Ct target − Ct GAPDH; ΔΔCt = ΔCt (CS) − ΔCt (CTRL); Gene expression level = $2^{-\Delta\Delta Ct}$. The following primers were used: GAPDH forward, 5′-AAG GTC GGA GTC AAG GGA TTT-3′, and reverse, 5′-AGA TGA TGA CCC TTT TGG CTC-3′; USP-19 forward, 5′-GGC ACA AGA TGA GGA ACG A-3′, and reverse, 5′-CAG ATA AAG GAA CGG GTC AA-3′; MHC forward, 5′-GCG GAA AGA AAG GTG GCA AGA-3′, and reverse, 5′-TGG GAA TGA GGC ATC GGA CAA-3′; myogenin forward, 5′-GCG GAA AGA AAG GTG GCA AGA-3′, and reverse, 5′-TGG GAA TGA GGC ATC GGA CAA-3′.

WESTERN BLOT ANALYSIS

Tissues and cells were harvested and lysed in lysis buffer (10 mM Tris-HCl, pH 7.4, 150 mM NaCl, 0.5% Nonidet P (NP)-40, 1 mM EDTA, 1 mM Na_3VO_4, and 1 mM PMSF). The protein concentration of each sample was determined by the BCA protein assay. Protein extracts made from the quadriceps femoris muscle (50 μg) and lysates of L6 myotubes (70 μg) were then subjected to standard sodium dodecyl sulfate-polyacrylamide gel electrophoresis (SDS-PAGE) and transferred to polyvinylidene fluoride (PVDF) membranes. After incubation with a blocking buffer [5% non-fat milk in 10 mM Tris-HCl, pH 7.5, 100 mM NaCl, 0.1% (w/v) Tween-20] for 2 h, the membranes were first incubated with antibody against GAPDH (1:1,000 dilution) (Sigma), USP-19 (1:200 dilution) (Santa Cruz Biotechnology), phospho-ERK1/2 (1:1,000 dilution), phospho-p38 (1:1,000 dilution), phospho-JNK (1:1,000 dilution), total ERK1/2 (1:1,000 dilution), p38 (1:1,000 dilution), JNK (1:1,000 dilution) (Cell Signaling Technology), or MHC (1:1,000 dilution) (Santa Cruz Biotechnology) overnight at 4°C, followed by a 1-h incubation with the appropriate secondary antibody conjugated to HRP. Detection was performed by enzyme-linked chemiluminescence (ECL). Relative quantities of proteins in western blotting were determined by scanning densitometry (ChemiDoc XRS+ Systems, Bio-Rad Laboratories, Inc.) and analyzed using Image Lab 2.0 Software (Bio-Rad Laboratories, Inc.). GAPDH was used as internal control for protein loading.

3-(4,5-DIMETHYLTHIAZOL-2-YL)-2,5-DIPHENYLTETRAZOLIUM BROMIDE (MTT) ASSAY

Cells were grown in 96-well plates at a density of 3×10^3 cells/well. Cells were exposed to control medium or medium containing various concentrations of CSE, 5 μM SB203580, 35 μM SP600125, and 10 μM PD98059. Cell survival was measured by the MTT assay 24 h later. Cells were stained with 20 μl sterile MTT dye (Sigma, 5 mg/ml) at 37°C for 4 h followed by removal of the culture medium and thorough mixing with 150 μl of dimethylsulfoxide (DMSO) for 10 min. Spectrometric absorbance was measured at 490 nm. Data are mean ± SE of three independent experiments performed in triplicate.

IMMUNOCYTOCHEMISTRY

Cells were seeded, incubated overnight on sterile cover glasses, and incubated with 20% CSE for 24 h after differentiation. Cells were washed with phosphate-buffered saline (PBS) and fixed with 4% paraformaldehyde. Following permeabilization in PBS containing 0.1% saponin, endogenous peroxidases were removed by 45-min incubation in peroxidase blocking solution (DAKO), and avidin and biotin were blocked using the Avidin/Biotin Blocking Kit. The cells were then stained with a rabbit polyclonal anti-smooth muscle actin (SMA) antibody (1:200 dilution) diluted in PBS overnight at 4°C. After washing in PBS, the cells were incubated with a goat anti-rabbit IgG/HRP antibody for 45 min at room temperature, followed by incubation with DAB peroxidase substrate. Counterstaining was done with hematoxylin. Images were acquired using an inverted Olympus CK40-F200 microscope.

ULTRASTRUCTURAL ANALYSIS UNDER TRANSMISSION ELECTRON MICROSCOPE (TEM)

L6 cells were treated with differentiation medium for 4 days, followed by 20% CSE for 24 h, and fixed with 3% glutaraldehyde at 4°C for 30 min. Using a modification of the method of Zhu et al. [2009], the fixed cells were collected using cell scrapers followed by a brief centrifugation. The cell pellets were fixed for an additional 2 h in 2% glutaraldehyde and 2 h in 1% osmium tetroxide. The cell pellets were dehydrated in an ascending ethanol series and embedded in Epon 618. Serial ultrathin sections were examined using a PHILIPS CM120 electron microscope. Magnifications 3,500× to 15,000×.

STATISTICAL ANALYSIS

Statistics were calculated with SPSS statistics v17.0 software. Student's *t* test was used for individual comparisons. Multiple comparisons were assessed by one-way ANOVA followed by Dunnett's tests. Differences between groups were considered significant at the $P < 0.05$ level. The results are presented as mean ± standard errors (SE).

RESULTS

CHRONIC EXPOSURE TO CS CAUSES THE UP-REGULATION OF USP-19 EXPRESSION IN THE QFM OF SD RATS

To determine the effects of cigarette smoke on USP-19 expression in skeletal muscle, we first measured USP-19 gene expression in the QFM of rats exposed to CS. All rats in the four groups survived the 12 weeks of study. Twelve weeks of CS exposure produced lung lesions that morphologically resembled human emphysema, which resulted in the enlargement of alveolar ducts (Fig. 1A). In addition, the mean ± SE bodyweights of the rats in the 4-, 8-, and 12-week CS exposure groups were 377 ± 2.27, 380 ± 3.61, and 366 ± 3.94 g, respectively. The mean bodyweights of the rats in the 8- and 12-week groups were lower than those in the control groups (400 ± 7.24, 411 ± 9.64), respectively (Fig. 1B, $P < 0.01$). Skeletal cell numbers per high-power (HP) lens increased after 12 weeks by 40% in comparison with the control group (Fig. 1C, $P < 0.05$), suggesting muscle wasting. Chronic CS exposure decreased the mRNA level of MHC in the 4-, 8-, and 12-week groups by 54, 81, and 89%, respectively (Fig. 1D). As shown in Figure 1E, MHC protein content in the QFM was decreased in the 8- and 12-week groups ($P < 0.05$). Taken together, these data indicate that muscle wasting

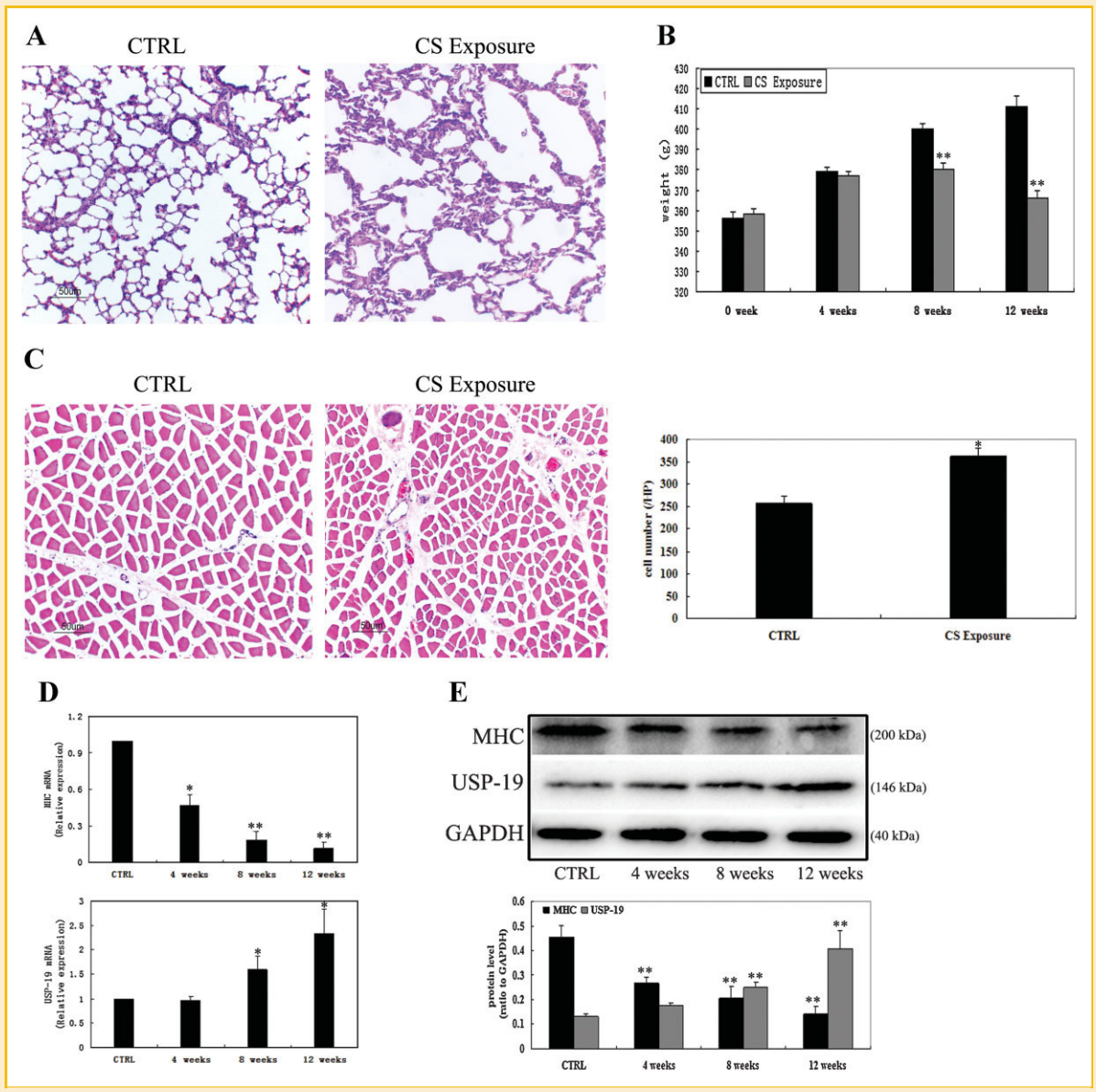

Fig. 1. Cigarette smoke exposure induces QFM wasting and increased USP-19 gene expression. (A) Cigarette smoke exposure-induced emphysema in SD rats. Photomicrographs of the lung from a control (CTRL) rat and a rat exposed to cigarette smoke for 12 weeks showed the typical pattern of emphysema: Alveolar ducts and enlarged alveoli (H&E, ×100). (B) Weight was determined at the indicated times. Each bar indicates the mean ± SE of the weights from three independent experiments. (C) Cell number per high-power (HP) lens in a skeletal muscle tissue section stained with H&E (×100). All fields shown are representative of multiple fields observed in three independent experiments. (D) MHC and USP-19 mRNA expression levels were assessed by qPCR. GAPDH served as the internal standard. Each bar indicates the mean ± SE from three independent experiments. (E) MHC and USP-19 protein were assessed by western blot analysis. GAPDH served as the control for sample loading. Optical density data from three independent experiments were analyzed by one-way ANOVA followed by Dunnett's multiple comparison test. $^{*}P < 0.05$ compared with CTRL; $^{**}P < 0.01$ compared with CTRL.

was induced by 8 and 12 weeks of CS exposure compared with untreated animals. Multiple qPCR analyses showed that USP-19 mRNA levels increased 60 or 133% after 8 (n = 6) or 12 weeks (n = 6) of exposure to CS, respectively, but were unchanged after 4 weeks (n = 6) (Fig. 1D). Western blot analysis was used to assess protein levels of USP-19. As shown in Figure 1E, USP-19 protein content was increased in the QFM from rats exposed to CS for 8 or 12 weeks ($P < 0.05$), and no significant changes were observed after 4 weeks of treatment.

CSE UP-REGULATES USP-19 GENE EXPRESSION IN L6 MYOTUBES

To evaluate the relationship between USP-19 expression and CS in vitro and understand the precise molecular mechanisms of the disorders triggered and regulated by CS at the cellular level, we measured changes in each parameter after exposing myotubes to CSE ranging from 5 to 20%. L6 cells were induced to differentiate in DMEM with 2% FBS for 4 days followed by 24 h of CSE treatment. USP-19 mRNA and protein were constitutively expressed in the control L6 myotubes, as shown in Figure 2A and B, respectively.

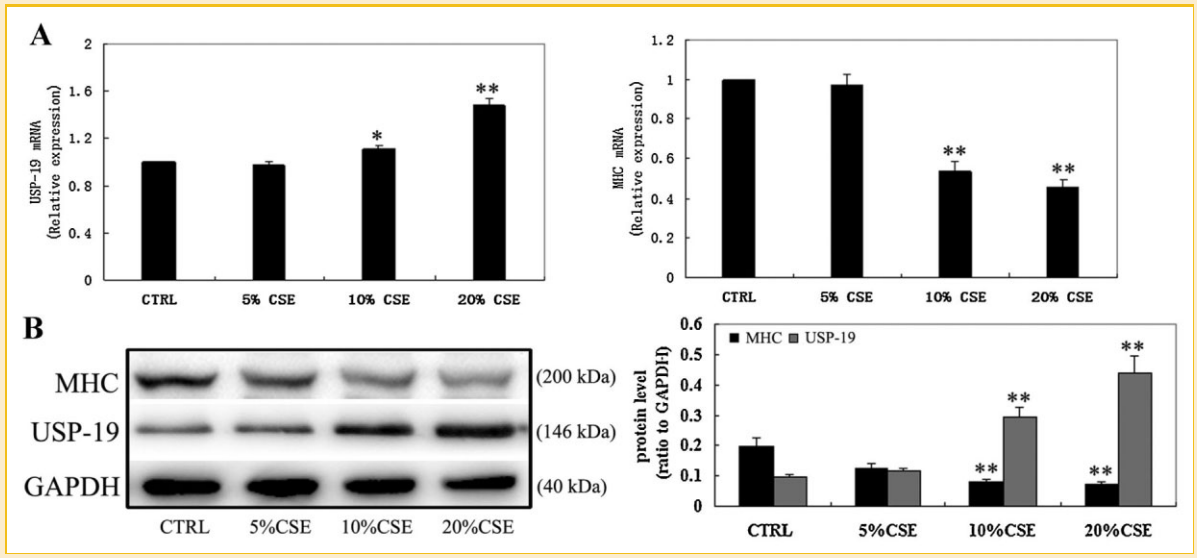

Fig. 2. CSE down-regulates MHC gene expression and up-regulates USP-19 gene expression in L6 myotubes. L6 myotubes were exposed to 5, 10, or 20% CSE for 24 h, then RNA and protein were extracted for qPCR and western blot analysis. (A) USP-19 and MHC mRNA levels were assessed by qPCR. GAPDH served as the internal standard. Each bar indicates the mean ± SE of normalized USP-19 and MHC mRNA from three independent experiments. (B) Western blotting for USP-19 and MHC protein. GAPDH served as the control for sample loading. Optical density data from three independent experiments were analyzed by one-way ANOVA followed by Dunnett's multiple comparison test. $^{*}P < 0.05$ versus control cells; $^{**}P < 0.01$ versus control cells.

After the cells were treated with CSE for 24 h, USP-19 mRNA level was significantly increased in a dose-dependent manner in the cells treated with 10 and 20% CSE by 10 and 48% (Fig. 2A); USP-19 protein content was increased in 10 and 20% CSE-treated L6 myotubes ($P < 0.05$). However, no significant changes were observed in the cells treated with 5% CSE. The up-regulation of USP-19 expression in L6 myotubes following CSE treatment is consistent with that found in the QFM tissue from CS-exposed rats.

CSE REDUCES MHC EXPRESSION AND MYOTUBE FORMATION

It is essential to understand the effect of CSE on L6 cells. Therefore, we examined the morphological changes in 20% CSE-treated L6 cells. L6 myotubes exhibited an elongated cell shape, were multi-nucleated, and even displayed fusion. The expression of smooth muscle actin (SMA) was detected by immunocytochemistry to identify myotubes (Fig. 3C). Compared with negative controls, SMA-stained myotubes were decreased in CSE-treated samples, suggesting decreased myotube fusion. To quantitate the wasting effect, we examined myogenin and MHC expression by qPCR (Figs. 3A and 2A) and western blot analysis (Fig. 2B). Compared with controls, MHC and myogenin mRNA levels were significantly lower after 10 and 20% CSE treatments, but not in the 5% CSE-treated cells. Ten and twenty percent CSE decreased myogenin mRNA expression by 40 and 43%, respectively; MHC mRNA expression by 46 and 55%, respectively. Lastly, transmission electron microscope (TEM) was performed to examine the ultrastructure of CSE-treated L6 cells (Fig. 3D). The L6 myotubes from the negative controls exhibited an abundance of myofibrils in the longitudinal sections and the characteristic arrangement of myofibrils in the transverse sections; however, muscle fibers were less numerous and shortened in CSE-treated L6 myotubes. In addition, cells were exposed to control medium or medium containing various concentrations of CSE. Cell survival was measured by the 3-(4,5-dimethylthiazol-2-yl)-2,5-diphenyltetrazolium bromide (MTT) assay 24 h later. CSE evoked a decrease in cell survival starting at a concentration of 30%. In contrast, the survival rates of cells treated with 5, 10, and 20% CSE had no change (Fig. 3B). Taken together, our results demonstrate that CSE causes muscle wasting in vitro by inhibiting myogenic differentiation and inducing the loss of myofibris.

CSE STIMULATES MAPK PHOSPHORYLATION

Myotube atrophy induced by TNF-α and H_2O_2 in C2C12 cells has been associated with the activation of MAPKs (in particular p38 MAPK) [Li et al., 2005]. To elucidate the signaling events by which CSE might regulate USP-19 gene expression, we systematically examined CSE's effects on MAPK activity in differentiated L6 cells. Western blot analysis using phosphospecific antibodies was performed to assess enzyme activation. L6 myotubes were exposed to 20% CSE for 24 h; then proteins were isolated and the levels of phosphorylated and total MAPKs were examined (Fig. 4). There were low levels of phosphorylated ERK1/2, p38, and JNK MAPKs in the control L6 myotubes. However, compared with the controls, 20% CSE significantly stimulated phosphorylation of ERK1/2, p38, and JNK without altering the total ERK1/2, p38, or JNK content. The effects of CSE on MAPKs were similar to those of TNF-α (20 ng/ml, a concentration shown to induce myotube protein loss) [Li et al., 2005; Magee et al., 2008] and lipopolysaccharide (LPS) (0.3 μg/ml).

ERK1/2 AND p38 MAPK INHIBITORS BLOCK CSE-MEDIATED USP-19 UP-REGULATION

To further evaluate whether the up-regulation of USP-19 in response to CSE occurred through MAPK phosphorylation, selected MAPK

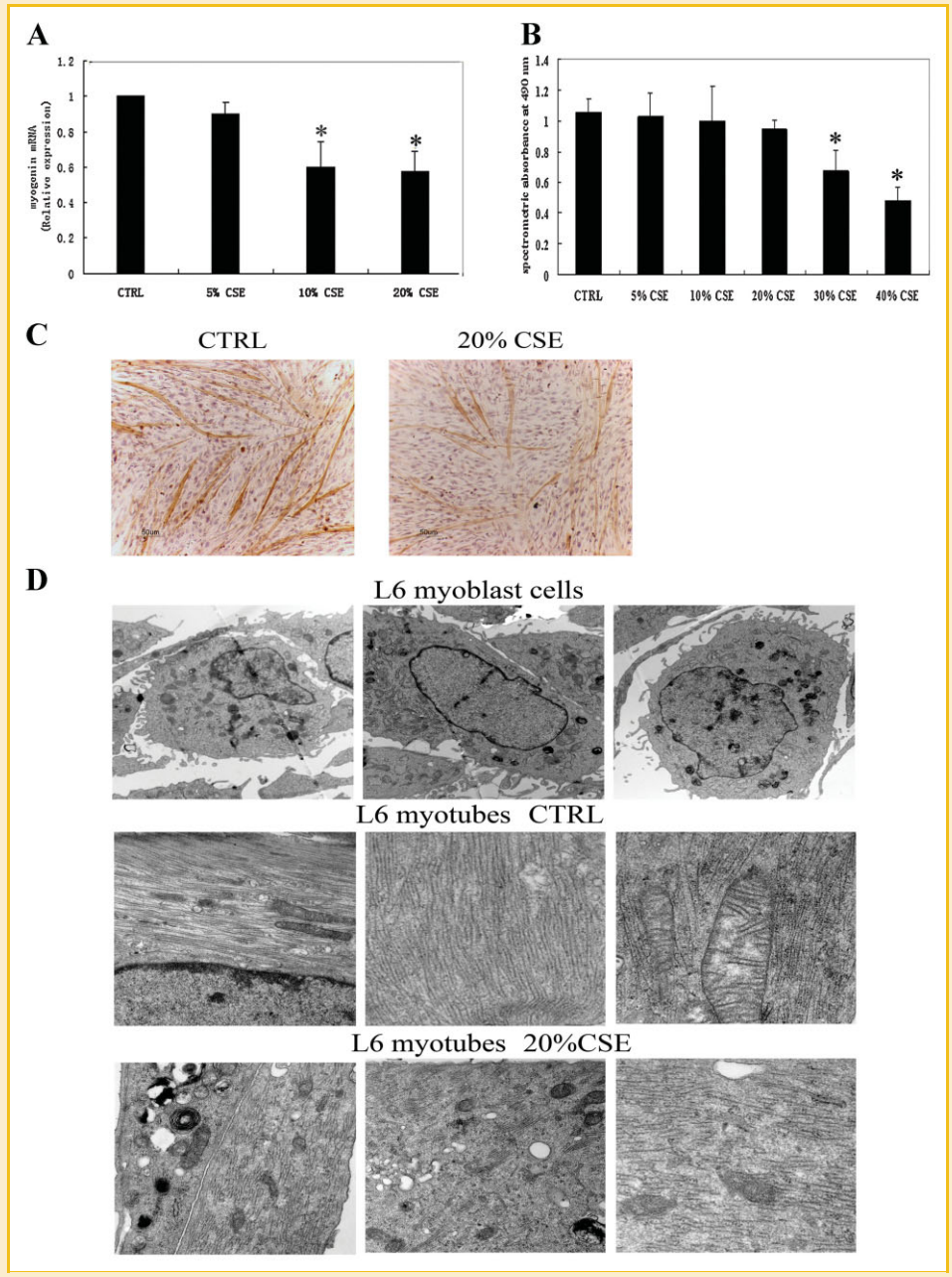

Fig. 3. CSE reduces MHC expression and myotube formation in L6 myotubes. L6 myotubes were cultured in the presence or absence of 20% CSE for 24 h. (A) Myogenin mRNA expression was analyzed by qPCR. Each bar indicates the mean ± SE of normalized myogenin mRNA from three independent experiments. GAPDH served as the internal standard. (B) Effects of CSE on L6 cell survival. L6 cells were treated with control medium or medium containing CSE (5, 10, 20, 30, 40%). Cell survival was measured by the 3-(4,5-dimethylthiazol-2-yl)-2,5-diphenyltetrazolium bromide (MTT) assay after 24 h. Each bar indicates the mean of spectrometric absorbance ± SE of three independent experiments performed in triplicate. (C) SMA expression was detected by immunocytochemistry (×100 magnification). All fields shown are representative of multiple fields observed in three independent experiments. (D) High magnification of electron micrographs showing the structures of L6 myotubes (×3,500–12,000). All fields shown are representative of multiple fields observed in three independent experiments. $^{*}P < 0.05$ versus control cells; $^{**}P < 0.01$ versus control cells.

inhibitors were used in this study. To test if the USP-19 up-regulation induced by CSE could be blocked by MAPKs inhibitors, L6 myotubes were pretreated for 30 min with the JNK inhibitor SP600125 (35 μM), the ERK inhibitor PD98059 (10 μM) or the p38 inhibitor SB203580 (5 μM) and exposed to 20% CSE for 24 h. Cell lysates were subjected to western blot analysis to detect for USP-19 (Fig. 5A). The pretreatment of L6 cells with ERK or p38 inhibitor blocked the elevated expression of USP-19 by CSE, suggesting that the ERK1/2 and p38 pathways may be involved in CSE mediated USP-19 up-regulation. On the contrary, the JNK inhibitor SP600125 and DMSO had no effect on USP-19 expression. In addition, cells were exposed to control medium or medium containing 5 μM

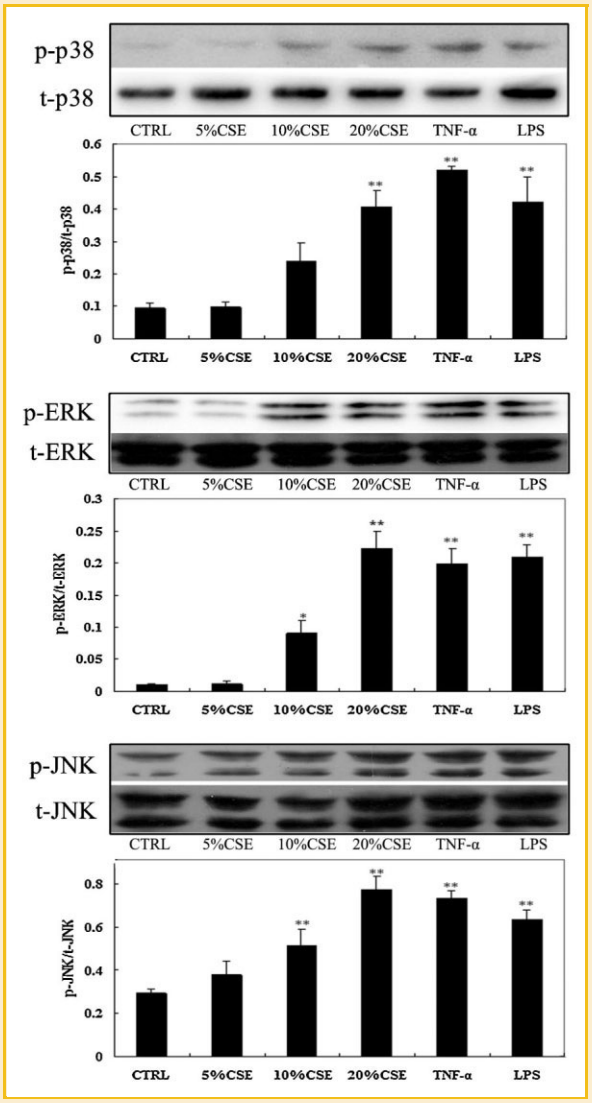

Fig. 4. CSE stimulates MAPKs phosphorylation in L6 myotubes. L6 myotubes were cultured in the presence or absence of 20% CSE for 24 h. Western blot analysis was performed using antibodies against either phosphorylated or non-phosphorylated ERK1/2, JNK, and p38 MAPK. The values for the expression of phospho-p38 MAPK, phospho-ERK, or phospho-JNK expressions were normalized to total-p38 MAPK, total-ERK, or total-JNK, respectively, are indicated on the bar graphs. Optical density data from three independent experiments were analyzed by one-way ANOVA followed by Dunnett's multiple comparison test. $^{*}P < 0.05$ versus control cells; $^{**}P < 0.01$ versus control cells.

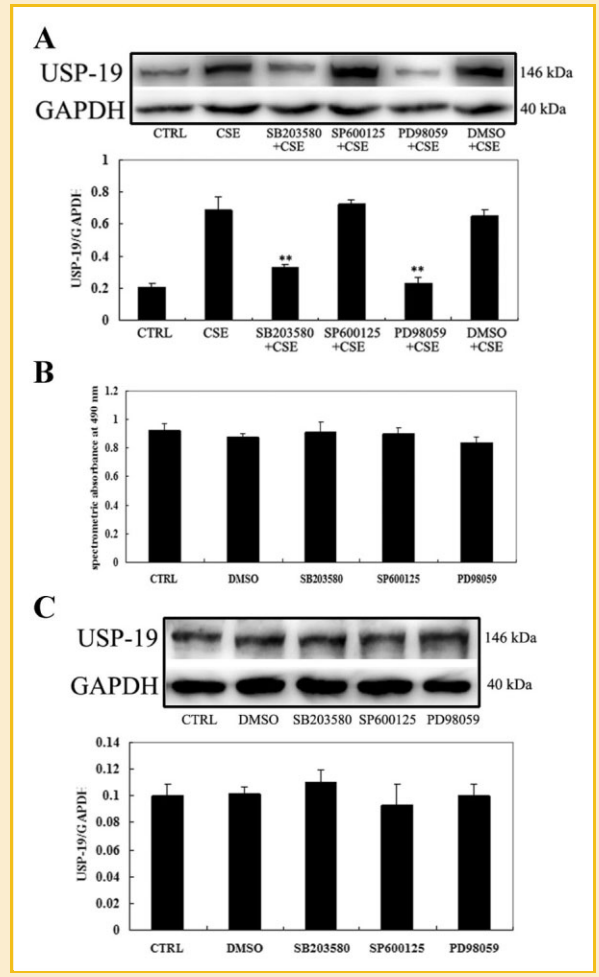

Fig. 5. ERK and p38 MAPK mediate CSE up-regulation of USP-19 gene expression. (A) L6 cells were preincubated with the JNK inhibitor SP600125 (35 μM), the ERK inhibitor PD98059 (10 μM) or the p38 inhibitor SB203580 (5 μM) for 30 min followed by 24 h incubation with 20% CSE. Total protein was extracted and analyzed by western blotting for USP-19 protein content. The values for USP-19 expression indicated on the bar graphs were normalized to GAPDH. Optical density data are representative of three independent experiments. $^{*}P < 0.05$ versus CSE. (B) Effects of MAPKs inhibitors on L6 cell survival. L6 cells were treated with control medium or medium containing 5 μM SB203580, 35 μM SP600125, and 10 μM PD98059. Cell survival rates were measured by MTT assay after 24 h. Each bar indicates the mean of spectrometric absorbance ± SE of three independent experiments performed in triplicate. (C) Western blot analysis using antibodies against USP-19 after treatment with MAPK inhibitors, respectively. GAPDH served as control for sample loading. The results are representative of three similar experiments. $^{*}P < 0.05$ versus control cells; $^{**}P < 0.01$ versus control cells.

SB203580, 35 μM SP600125, and 10 μM PD98059. Cell survival rats were measured by MTT assay 24 h later. MAPK inhibitor alone has no effect on cell survival (Fig. 5B). As Figure 5C shows, L6 cells were exposed to control medium or medium containing 5 μM SB203580, 35 μM SP600125, and 10 μM PD98059 and western blot analysis was used to assess protein expression of USP-19 24 h later. The increase of USP-19 expression caused by the p38 inhibitor SB203580 and the decrease of USP-19 expression caused by the JNK inhibitor SP600125 are only slightly, but no significantly. Neither DMSO nor the ERK inhibitor PD98059 had any effect on USP-19 expression.

CHRONIC EXPOSURE TO CS STIMULATES p38 AND ERK1/2 PHOSPHORYLATION IN THE QFM OF RATS

Rats were exposed to cigarette smoke for 12 weeks, and sham-exposed animals were exposed to normal air under the same conditions. The effects of CS exposure on p38 and ERK phosphorylation were tested by western blot analysis. As shown in Figure 6, marked phosphorylation of p38 and ERK1/2 occurred in the QFM of rats exposed to CS. The change of ERK activity is consistent with a report by Penna et al. [2010] showing that marked

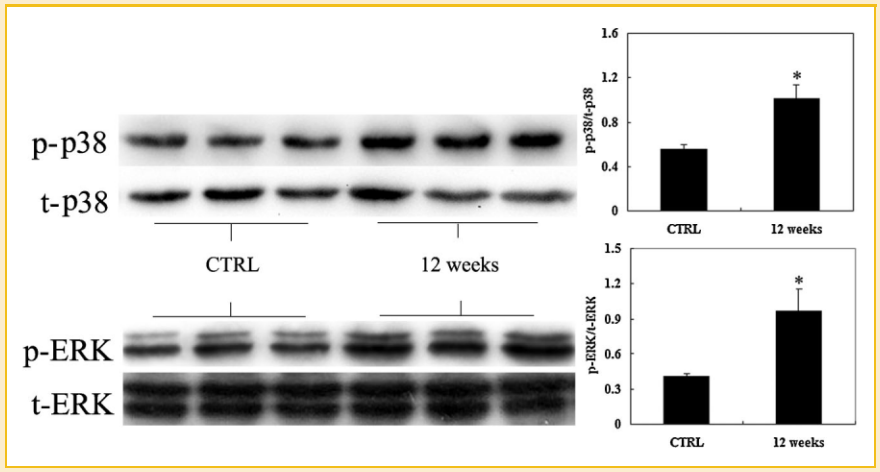

Fig. 6. Twelve weeks CS exposure stimulates p38 and ERK1/2 phosphorylation in the QFM of rats. Rats were exposed to chronic CS. Western blotting used to quantify the total or phosphorylated amounts of p38 and ERK1/2 present in the QFM of rats. The optical density data from three independent experiments were analyzed by Student's *t* test. $^{*}P < 0.05$ versus CTRL; $^{**}P < 0.01$ versus CTRL.

phosphorylation of ERK1/2 occurs in the skeletal muscles of tumor-bearing rats.

DISCUSSION

COPD results in significant systemic effects, among which muscle dysfunction/wasting is one of the most important. Muscle atrophy results primarily from accelerated protein degradation via the ubiquitin–proteasome pathway [Lecker et al., 1999]. Ubiquitination is controlled by the balance of ubiquitinating and deubiquitinating enzymes (DUBs). Despite the numerous DUBs encoded by the human genome and their implication in numerous cellular functions [Reyes-Turcu et al., 2009], the physiological functions of most of these enzymes remain largely unknown.

We obtained evidence that the expression of the USP-19 deubiquitinating enzyme is regulated in animal models of COPD induced by CS. To induce COPD, different groups of rats were exposed to CS. Twelve weeks of CS exposure produced emphysema, and both 8 and 12 weeks of CS exposure induced significant weight loss and decreases in muscle size. Similar to our results, chronic exposure to the smoke of 10 cigarettes per day for 16 weeks induced lung parenchymal destruction, enlargement of air-spaces, and loss of bodyweight in rats [Lee et al., 2005]. We show that MHC in the QFM at the protein and mRNA level is decreased by exposure to CS, suggesting that muscle wasting occurs during CS exposure. Factors considered potentially relevant to skeletal muscle dysfunction induced by CS include hypoxia, hypercapnia, nutritional depletion, anabolic/catabolic hormone imbalance, systemic or local inflammation, and oxidative stress [Man et al., 2009]. Ubiquitin–proteasome pathway components, such as E3 ligase proteins (MAFbx and MuRF1), are up-regulated by a variety of factors that are relevant to muscle dysfunction in COPD, such as muscle inactivity, pro-inflammatory cytokines and reactive oxygen species [Gomes et al., 2001]. The present study demonstrated that CS could also stimulate the expression of the deubiquitinating enzyme USP-19 gene. Eight and 12 weeks of CS exposure up-regulate USP-19 expression levels in the QFM of rats. Furthermore, USP-19 expression is negatively correlated with weight, muscle size, and MHC level and positively correlated with the length of CS exposure; these results suggest that USP-19 acts as a negative regulator in catabolic muscles similar to USP-14, a deubiquitinating enzyme associated with muscle atrophy [Lecker et al., 2004]. The changes in USP-19 that we observed are consistent with the report by Combaret et al. [2005] that USP-19 is up-regulated in atrophying rat skeletal muscle in response to fasting, streptozotocin-induced diabetes, dexamethasone treatment, or cancer; high USP-19 mRNA levels have been associated with low muscle mass.

Evidence that CS induces muscle wasting is obtained from the studies involving animals. Subsequently, we demonstrate that CSE has direct effects within cells and investigate the precise molecular mechanisms of the disorders triggered by CS at the cellular level. We examined the effect of CSE on L6 myotubes. The ultrastructural features observed in CSE-treated L6 cells changed: the muscle fibers decreased in number, and the length of muscle fibers in the longitudinal sections shortened. These findings were likely due to defective differentiation. Indeed, staining for SMA by immunocytochemistry showed decreased fusion fields. Furthermore, compared with controls, MHC and myogenin mRNA levels were significantly lower after 10 and 20% CSE treatments. Muscle cell differentiation is strictly regulated by the myogenic transcription factor family [Davie et al., 2007], particularly myogenin in the L6 myotubes [Myer et al., 2001], and the absence of myogenin reduces MHC expression and myotube formation. Our results suggest that CSE inhibits myogenic differentiation and myotube formation. Furthermore, accelerated MHC protein loss suggested that CSE could inhibit the synthesis of MHC. In contrast, 10 and 20% CSE up-regulated USP-19 mRNA and protein level which is consistent with our results in the QFM tissue from CS-exposed rats. The USP-19 gene is constitutively expressed in differentiated myotubes and adult rat skeletal muscle, suggesting that it plays a physiological role in regulating protein turnover. MHC and USP-19 expression were negatively correlated. A recent report

by Sundaram et al. [2009] shows that depletion of USP-19 acts at the level of gene transcription to increase the expression of MHC in myotubes in culture. In addition, depletion of USP-19 increases myogenin gene expression in L6 myotubes, increases the extent of muscle cell fusion, and regulates the expression of MHC in a myogenin-dependent manner. As described above, CSE negatively affected the differentiation of L6 myotubes partly by decreasing myogenin and up-regulating USP-19. Together, these findings indicate a causal link between USP-19 activation and inhibition of myogenic differentiation. Our current study also suggests that the CSE evoked a decrease in cell survival starting at a concentration of 30%; in contrast, the survival rate of cells treated with 20% CSE had no change. However, at this time, we cannot exclude the possibility that the wasting induced by CSE may be associated with the increased degradation or degeneration of myotubes. In addition to resulting from the balance between anabolism and catabolism or the regulation of muscle differentiation, muscle wasting may be the consequence of a decreased number of fibers resulting from the activation of apoptotic pathways, which is an attractive possibility for future investigation. Our results also suggest that CSE-treated L6 cells may act as models of muscle wasting in vitro. Oxygen free radical-treated or TNF-α-treated myotubes are frequently used as in vitro models of muscle wasting [Spiegelman and Hotamisligil, 1993; Hansen et al., 2007; Russell et al., 2010]. Considering that CSE contains various oxygen free radicals and induces overexpression and secretion of TNF-α in type II pneumocytes [Lixuan et al., 2010] and HaCaT human keratinocytes [Jeong et al., 2010], we will evaluate the level of inflammatory cytokines (e.g., TNF-α and interleukin-1 and -6) with CSE treatment in the future to explore the mechanisms by which CSE induces myotube atrophy in L6 myotubes. However, the CSE prepared in this study only contained the hydrophilic components of cigarette smoke. The extent of USP-19 expression in L6 myotubes was not comparable to those of animal studies in vivo because of the different preparations of CS and CSE used. In addition, in vitro CSE exposure is different from in vivo cigarette smoking because the former bypasses the airways and precludes the filtering action of the lungs. Thus, further studies are needed to elucidate additional effects of CSE and their mechanisms. These investigations need to be taken into account when cultured myotubes are used in future studies of muscle wasting.

Our findings suggest that CSE may contribute to muscle wasting through the inhibition of myogenic differentiation by a USP-19-dependent pathway aimed at uncovering the molecular mechanisms that regulate the level of USP-19 that could provide insight into ways of suppressing CS-induced muscle atrophy are therefore warranted. We find that 20% CSE activated all three major MAPK signaling pathways in L6 myotubes after 24 h incubation, which is consistent with the observation by Pera et al. [2010] that constitutive phosphorylation of MAPKs is induced by CSE in the airway smooth muscle. TNF-α activated three MAPK signaling pathways in L6 myotubes similarly to the effect obtained by Li et al. [2005] in C2C12 myotubes. Inhibitor studies showed that SB203580 and PD98059 inhibited the up-regulation of USP-19 induced by CSE, however inhibitors alone had no significant effect on it. We considered that the activation of MAPKs induced by CSE might result from components such as LPS, oxygen free radicals and the secretion of TNF-α. The mechanisms of attenuation of muscle protein degradation induced by TNF-α and oxygen free radicals are related to p38 MAPK [Li et al., 2005, 2007]. The activity of p38 favors protein degradation and muscle atrophy. We measured p38 and ERK1/2 activity in the QFM of rats exposed to CS. The results revealed that marked phosphorylation of p38 and ERK1/2, which is involved in USP-19 regulation in CSE-treated L6 myotubes, occurs in CS-exposed rats. Our current results suggest that CS-induced muscle wasting is caused partly by p38 and ERK1/2 signaling, and that the USP-19 gene plays a crucial role in its pathogenesis. In this regard, previous studies have reported that many catabolic conditions, including type 2 diabetes [Koistinen et al., 2003], aging [Williamson et al., 2003] and acute quadriplegic myopathy [Di Giovanni et al., 2004] show an elevation of p38 phosphorylation in skeletal muscle. Enhanced activity of ERK1/2 occurs in wasting muscles during the course of experimental cancer cachexia [Penna et al., 2010].

In summary, the present data provide novel evidence that following CS treatment, myoblast differentiation is dramatically inhibited (reduced MHC, myogenin, and extent of muscle cell fusion). An attractive possibility is that USP-19 contributes to the muscle wasting induced by CS. CSE increases USP-19 expression via the p38 and ERK pathways. Gaining more insight into the functions and mechanisms of action of USP-19 is crucial for the development of new and individualized therapeutic strategies to prevent skeletal muscle dysfunction/wasting in COPD patients.

ACKNOWLEDGMENTS

This research was supported by funds from Shanghai Natural Science Foundation (SNSF) Project (Contract grant number: 05ZR14063). The authors thank all members of their laboratory for helpful discussion.

REFERENCES

Bodine SC, Latres E, Baumhueter S, Lai VK, Nunez L, Clarke BA, Poueymirou WT, Panaro FJ, Na E, Dharmarajan K, Pan ZQ, Valenzuela DM, DeChiara TM, Stitt TN, Yancopoulos GD, Glass DJ. 2001. Identification of ubiquitin ligases required for skeletal muscle atrophy. Science 294:1704–1708.

Carp H, Janoff A. 1978. Possible mechanisms of emphysema in smokers. In vitro suppression of serum elastase-inhibitory capacity by fresh cigarette smoke and its prevention by antioxidants. Am Rev Respir Dis 118:617–621.

Churg A, Cosio M, Wright JL. 2008. Mechanisms of cigarette smoke-induced COPD: Insights from animal models. Am J Physiol Lung Cell Mol Physiol 294:612–631.

Ottenheijm CAC, Heunks LMA, Dekhuijzen RPN, Lopez AD, Murray CC. 1998. The global burden of disease, 1990–2020. Nat Med 4:1241–1243.

Combaret L, Adegoke OA, Bedard N, Baracos V, Attaix D, Wing SS. 2005. USP19 is a ubiquitin-specific protease regulated in rat skeletal muscle during catabolic states. Am J Physiol Endocrinol Metab 288:693–700.

Coulthard LR, White DE, Jones DL, McDermott MF, Burchill SA. 2009. P38 MAPK: Stress responses from molecular mechanisms to therapeutics. Trends Mol Med 15:369–379.

Davie JK, Cho JH, Meadows E, Flynn JM, Knapp JR, Klein WH. 2007. Target gene selectivity of the myogenic basic helix-loop-helix transcription factor myogenin in embryonic muscle. Dev Biol 311:650–664.

Decramer M, Gosselink R, Troosters T, Verschueren M, Evers G. 1997. Muscle weakness is related to utilization of health care resources in COPD patients. Eur Respir J 10:417–423.

Di Giovanni S, Molon A, Broccolini A, Melcon G, Mirabella M, Hoffman EP, Servidei S. 2004. Constitutive activation of MAPK cascade in acute quadriplegic myopathy. Ann Neurol 55:195–206.

Doucet M, Russell AP, Léger B, Debigaré R, Joanisse DR, Caron MA, LeBlanc P, Maltais F. 2007. Muscle atrophy and hypertrophy signaling in patients with chronic obstructive pulmonary disease. Am J Respir Crit Care Med 176:261–269.

Gomes MD, Lecker SH, Jagoe RT, Navon A, Goldberg AL. 2001. Atrogin-1, a muscle-specific F-box protein highly expressed during muscle atrophy. Proc Natl Acad Sci USA 98:14440–14445.

Hansen JM, Klass M, Harris C, Csete M. 2007. A reducing redox environment promotes C2C12 myogenesis: Implications for regeneration in aged muscle. Cell Biol Int 31:546–553.

Jagoe RT, Lecker SH, Gomes M, Goldberg AL. 2002. Patterns of gene expression in atrophying skeletal muscles: Response to food deprivation. FASEB J 16:1697–1712.

Jeong SH, Park JH, Kim JN, Park YH, Shin SY, Lee YH, Kye YC, Son SW. 2010. Up-regulation of TNF-alpha secretion by cigarette smoke is mediated by Egr-1 in HaCaT human keratinocytes. Exp Dermatol 19:206–212.

Koistinen HA, Chibalin AV, Zierath JR. 2003. Aberrant p38 mitogen-activated protein kinase signaling in skeletal muscle from Type 2 diabetic patients. Diabetologia 46:1324–1328.

Lecker SH, Solomon V, Mitch WE, Goldberg AL. 1999. Muscle protein breakdown and the critical role of the ubiquitin-proteasome pathway in normal and disease states. J Nutr 129:227–237.

Lecker SH, Jagoe RT, Gilbert A, Gomes M, Baracos V, Bailey J, Price SR, Mitch WE, Goldberg AL. 2004. Multiple types of skeletal muscle atrophy involve a common program of changes in gene expression. FASEB J 18:39–51.

Lee JH, Lee DS, Kim EK, Choe KH, Oh YM, Shim TS, Kim SE, Lee YS, Lee SD. 2005. Simvastatin inhibits cigarette smoking-induced emphysema and pulmonary hypertension in rat lungs. Am J Respir Crit Care Med 172:987–993.

Lixuan Z, Jingcheng D, Wenqin Y, Jianhua H, Baojun L, Xiaotao F. 2010. Baicalin attenuates inflammation by inhibiting NF-kappaB activation in cigarette smoke induced inflammatory models. Pulm Pharmacol Ther 23: 411–419.

Li W, Xu YJ, Shen HH. 2007. Effect of cigarette smoke extract on lipopolysaccha-ride-activated mitogen-activated protein kinase signal transduction pathway in cultured cells. Chin Med J 120:1075–1081.

Li YP, Chen Y, John J, Moylan J, Jin B, Mann DL, Reid MB. 2005. TNF-alpha acts via p38 MAPK to stimulate expression of the ubiquitin ligase atrogin1/MAFbx in skeletal muscle. FASEB J 19:362–370.

Magee P, Pearson S, Allen J. 2008. The omega-3 fatty acid, eicosapentaenoic acid (EPA), prevents the damaging effects of tumour necrosis factor (TNF)-alpha during murine skeletal muscle cell differentiation. Lipids Health Dis 7:24.

Man WD, Kemp P, Moxham J, Polkey MI. 2009. Skeletal muscle dysfunction in COPD: Clinical and laboratory observations. Clin Sci (Lond) 117:251–264.

Myer A, Olson EN, Klein WH. 2001. MyoD cannot compensate for the absence of myogenin during skeletal muscle differentiation in murine embryonic stem cells. Dev Biol 229:340–350.

Pera T, Gosens R, Lesterhuis AH, Sami R, Toorn M, Zaagsma J, Meurs H. 2010. Cigarette smoke and lipopolysaccharide induce a proliferative airway smooth muscle phenotype. Respir Res 11:48.

Penna F, Costamagna D, Fanzani A, Bonelli G, Baccino FM, Costelli P. 2010. Muscle wasting and impaired myogenesis in tumor bearing mice are prevented by ERK inhibition. PloS One 5:e13640.

Reyes-Turcu FE, Ventii KH, Wilkinson KD. 2009. Regulation and cellular roles of ubiquitin-specific deubiquitinating enzymes. Annu Rev Biochem 78:363–397.

Russell ST, Siren PM, Siren MJ, Tisdale MJ. 2010. Mechanism of attenuation of protein loss in murine C2C12 myotubes by D-myo-inositol 1,2,6-triphosphate. Exp Cell Res 316:286–295.

Sacheck JM, Hyatt JP, Raffaello A, Jagoe RT, Roy RR, Edgerton VR, Lecker SH, Goldberg AL. 2007. Rapid disuse and denervation atrophy involve transcriptional changes similar to those of muscle wasting during systemic diseases. FASEB J 21:140–155.

Shih RH, Lee IT, Hsieh HL, Kou YR, Yang CM. 2010. Cigarette smoke extract induces HO-1 expression in mouse cerebral vascular endothelial cells: Involvement of c-Src/NADPH oxidase/PDGFR/JAK2/STAT3 pathway. J Cell Physiol 225:741–750.

Spiegelman BM, Hotamisligil GS. 1993. Through thick and thin: Wasting, obesity, and TNF alpha. Cell 73:625–627.

Stevenson CS, Coote K, Webster R, Johnston H, Atherton HC, Nicholls A, Giddings J, Sugar R, Jackson A, Press NJ, Brown Z, Butler K, Danahay H. 2005. Characterization of cigarette smoke-induced inflammatory and mucus hypersecretory changes in rat lung and the role of CXCR2 ligands in mediating this effect. Am J Physiol Lung Cell Mol Physiol 288:L514–L522.

Sultan KR, Henkel B, Terlou M, Haagsman HP. 2006. Quantification of hormone-induced atrophy of large myotubes from C2C12 and L6cells: Atrophy-inducible and atrophy-resistant C2C12 myotubes. Am J Physiol Cell Physiol 290:650–659.

Sundaram P, Pang Z, Miao M, Yu L, Wing SS. 2009. USP19-deubiquitinating enzyme regulates levels of major myofibrillar proteins in L6 muscle cells. Am J Physiol Endocrinol Metab 297:1283–1290.

Tracey KJ. 2002. Lethal weight loss: The focus shifts to signal transduction. Sci STKE 2002:pe21.

Williamson D, Gallagher P, Harber M, Hollon C, Trappe S. 2003. Mitogen-activated protein kinase (MAPK) pathway activation: Effects of age and acute exercise on human skeletal muscle. J Physiol 547:977–987.

Zhu GH, Huang J, Bi Y, Su Y, Tang Y, He BC, He Y, Luo J, Wang Y, Chen L, Zuo GW, Jiang W, Luo Q, Shen J, Liu B, Zhang WL, Shi Q, Zhang BQ, Kang Q, Zhu J, Tian J, Luu HH, Haydon RC, Chen Y, He TC. 2009. Activation of RXR and RAR signaling promotes myogenic differentiation of myoblastic C2C12cells. Differentiation 78:195–204.